Field intensity distributions and polarization orientations in a vacuum-clad subwavelength-diameter optical fiber

Fam Le Kien [a,*,1], J.Q. Liang [a], K. Hakuta [a], V.I. Balykin [a,b]

[a] *Department of Applied Physics and Chemistry, University of Electro-Communications, 1-5-1 Chofugaoka, Chofushi, Tokyo 182-8585, Japan*
[b] *Institute of Spectroscopy, Troitsk, Moscow Region 142092, Russia*

Abstract

We study the properties of the field in the fundamental mode HE_{11} of a vacuum-clad *subwavelength-diameter* optical fiber using the exact solutions of Maxwell's equations. We obtain simple analytical expressions for the total intensity of the electric field. We discuss the origin of the deviations of the exact fundamental mode HE_{11} from the approximate mode LP_{01}. We show that the thin thickness of the fiber and the high contrast between the refractive indices of the silica core and the vacuum-clad substantially modify the intensity distributions and the polarization properties of the field and its components, especially in the vicinity of the fiber surface. One of the promising applications of the field around the subwavelength-diameter fiber is trapping and guiding of atoms by the optical force of the evanescent field.
© 2004 Published by Elsevier B.V.

1. Introduction

Optical fibers with diameters from micrometers to millimeters have found many important applications in technology. The guiding properties of such fibers have been well studied [1]. Most fibers use core and cladding materials with nearly the same refractive indices. Such fibers are referred to as weakly guiding fibers. The description of weakly guiding fibers is greatly simplified due to the use of the linearly polarized (LP) modes, which are approximate solutions of Maxwell's equations and are superpositions of two corresponding nearly degenerate eigenmodes.

---

* Corresponding author. Tel.: +81 424 43 5476; fax: +81 424 43 5507.

E-mail address: fam@kiji.pc.uec.ac.jp (F.L. Kien).

[1] Also at Institute of Physics and Electronics, Vietnamese Academy of Science and Technology, Hanoi, Vietnam.

Recently, thin waveguides have become attractive for a wide range of potential practical applications. It has been pointed out that the intense evanescent field in the vicinity of a tapered fiber can be used as an atomic mirror [2]. Generation of light with a supercontinuum spectrum in a thin tapered fiber has been demonstrated [3]. The evanescent waves from zero-mode metal-clad subwavelength-diameter waveguides have been used for optical observations of single-molecule dynamics [4]. Several types of dielectric submicrometer- and nanometer-diameter wire waveguides have been fabricated, and their guiding properties have been investigated [5]. It has been proposed to use the optical force of an evanescent wave around a thin fiber for atom trapping and guiding [6]. Thin fiber structures can be used as building blocks in the future micro- and nano-photonic devices.

Unlike the case of optical fibers with diameter larger than the wavelength, many properties of subwavelength-diameter fibers have not been adequately investigated. In such a thin fiber, the original silica core is vanishing. Therefore, the original silica-clad acts like a core while the surrounding vacuum (or air) acts like a clad. Due to the high refractive index contrast between the silica core and the vacuum-clad, the description of subwavelength-diameter fibers in terms of weakly guided LP modes is questionable. It has been demonstrated that such fibers have interesting properties such as high power density at the fiber surface and cylindrical asymmetry in the field distribution [2], large penetration length of the evanescent wave [6], enhancement of the power fraction of the field outside the fiber [6,7], and large waveguide dispersion [7]. However, the intensity distributions and polarization orientations of the fields in subwavelength-diameter fibers have not been studied.

In this paper, we study the field intensity distributions and polarization orientations in the fundamental mode HE_{11} of a vacuum-clad *subwavelength-diameter* optical fiber using the *exact* solutions of Maxwell's equations. We show that the thin thickness of the fiber and the high contrast between the refractive indices of the silica core and the vacuum-clad substantially modify the intensity distributions and the polarization orientations of the field and its components. The study

of such properties is necessary not only for academic interest but also for practical applications such as trapping of atoms by the optical force of an evanescent wave around a thin fiber [6].

Before we proceed, we note that, in related problems, the decay of an atom in the presence of a fiber was considered for the first time by Katsenelenbaum in 1949 [8]. Excitation of fiber modes with a dipole source and influence of a fiber on the decay rate of a single atom were investigated in [8–11]. In the present paper, we do not consider how the modes can be excited. Due to the adiabatic tapping condition [12], the fundamental mode HE_{11} of a subwavelength-diameter fiber can be excited by the standard coupling techniques [5].

The paper is organized as follows. In Section 2, we describe the general model of a thin fiber and examine a fundamental mode with quasi-linear polarization. In Section 3, we study a fundamental mode with rotating (circulating) polarization. Our conclusions are given in Section 4.

2. Thin fiber and fundamental mode with quasi-linear polarization

Consider a thin single-mode optical fiber that has a cylindrical silica core of radius a and refractive index n_1 and an infinite vacuum-clad of refractive index $n_2 = 1$. Such a fiber can be prepared using taper fiber technology. The essence of the technology is to heat and pull a single-mode optical fiber to a very thin thickness maintaining the taper condition to keep adiabatically the single-mode condition [3,12]. Due to tapering, the original core is almost vanishing. Therefore, the refractive indices that determine the guiding properties of the tapered fiber are the refractive index of the original silica-clad and the refractive index of the surrounding vacuum. The refractive index and the radius of the tapered silica-clad will be henceforth referred to simply as the fiber refractive index n_1 and the fiber radius a, respectively.

We send a light of wavelength λ, frequency ω, and free-space wave number $k = 2\pi/\lambda = \omega/c$ through the fiber. Under the condition $V \equiv ka\sqrt{n_1^2 - n_2^2} < V_c \cong 2.405$, the fiber can support only one mode, referred to as the fundamen-

tal mode HE_{11}. The longitudinal propagation constant β of this mode is determined by the eigenvalue equation [1]

$$
\frac{J_0(ha)}{haJ_1(ha)} = -\frac{n_1^2 + n_2^2}{2n_1^2}\frac{K_1'(qa)}{qaK_1(qa)} + \frac{1}{h^2a^2}
$$
$$
- \left\{\left[\frac{n_1^2 - n_2^2}{2n_1^2}\frac{K_1'(qa)}{qaK_1(qa)}\right]^2\right.
$$
$$
\left. + \frac{\beta^2}{n_1^2k^2}\left(\frac{1}{q^2a^2} + \frac{1}{h^2a^2}\right)^2\right\}^{1/2}. \qquad (1)
$$

Here the parameters $h = (n_1^2k^2 - \beta^2)^{1/2}$ and $q = (\beta^2 - n_2^2k^2)^{1/2}$ characterize the fields inside and outside the fiber. The notation J_n and K_n stand for the Bessel functions of the first kind and the modified Bessel functions of the second kind, respectively.

We first study a fundamental mode with quasi-linear polarization. In the cylindrical coordinates (r, φ, z), the solutions of Maxwell's equations for the Cartesian components of the electric field **E** in such a mode are given, for $r < a$ (inside the fiber), by [1]

$$
E_x = -iA\frac{\beta}{2h}[(1-s)J_0(hr)\cos\varphi_0
$$
$$
- (1+s)J_2(hr)\cos(2\varphi-\varphi_0)]e^{i(\omega t-\beta z)},
$$
$$
E_y = -iA\frac{\beta}{2h}[(1-s)J_0(hr)\sin\varphi_0 \qquad (2)
$$
$$
- (1+s)J_2(hr)\sin(2\varphi-\varphi_0)]e^{i(\omega t-\beta z)},
$$
$$
E_z = AJ_1(hr)\cos(\varphi-\varphi_0)e^{i(\omega t-\beta z)},
$$

and, for $r > a$ (outside the fiber), by [1]

$$
E_x = -iA\frac{\beta}{2q}\frac{J_1(ha)}{K_1(qa)}[(1-s)K_0(qr)\cos\varphi_0
$$
$$
+ (1+s)K_2(qr)\cos(2\varphi-\varphi_0)]e^{i(\omega t-\beta z)},
$$
$$
E_y = -iA\frac{\beta}{2q}\frac{J_1(ha)}{K_1(qa)}[(1-s)K_0(qr)\sin\varphi_0 \qquad (3)
$$
$$
+ (1+s)K_2(qr)\sin(2\varphi-\varphi_0)]e^{i(\omega t-\beta z)},
$$
$$
E_z = A\frac{J_1(ha)}{K_1(qa)}K_1(qr)\cos(\varphi-\varphi_0)e^{i(\omega t-\beta z)},
$$

where $s = [(qa)^{-2} + (ha)^{-2}]/[J_1'(ha)/haJ_1(ha) + K_1'(qa)/qaK_1(qa)]$. The coefficient A is determined by the normalization condition. The angle φ_0 determines the orientation axis of the polarization of

the field. The two sets of solutions corresponding to $\varphi_0 = 0$ and $\pi/2$ express two different polarizations, aligned along the x and y axes, respectively.

For practical applications such as trapping of atoms by the optical force of an evanescent wave around a thin fiber [6], it is necessary to calculate the optical potential, which is proportional to the total intensity $|E|^2$ of the electric field. A rigorous expression for $|E|^2$ can be easily obtained with the help of Eqs. (2) and (3). For $r < a$, we find

$$
|E|^2 = g_{in}\{J_0^2(hr) + uJ_1^2(hr) + fJ_2^2(hr) + [uJ_1^2(hr)
$$
$$
- f_pJ_0(hr)J_2(hr)]\cos[2(\varphi-\varphi_0)]\}. \qquad (4)
$$

For $r > a$, we get

$$
|E|^2 = g_{out}\{K_0^2(qr) + wK_1^2(qr) + fK_2^2(qr)
$$
$$
+ [wK_1^2(qr) + f_pK_0(qr)K_2(qr)]
$$
$$
\times \cos[2(\varphi-\varphi_0)]\}. \qquad (5)
$$

Here we have introduced the parameters $u = 2h^2/\beta^2(1-s)^2$, $w = 2q^2/\beta^2(1-s)^2$, $f = (1+s)^2/(1-s)^2$, and $f_p = 2(1+s)/(1-s)$. We have also introduced the notation $g_{in} = |A|^2/2u$ and $g_{out} = |A|^2J_1^2(ha)/2wK_1^2(qa)$. The terms $J_0^2(hr)$ and $K_0^2(qr)$ in the expressions (4) and (5), respectively, correspond to the total intensity of the electric field in the mode LP_{01}. The other terms describe the deviations of the exact mode HE_{11} from the approximate mode LP_{01}.

The above expressions are mathematically valid for any core radius a and any pair of refractive indices n_1 and n_2 where $n_1 > n_2$. Before applying these expressions to thin tapered fibers, we recall the case of conventional single-mode fibers, where $\Delta \equiv (n_1 - n_2)/n_1 \ll 1$ and $a > \lambda$. In this case, we have [1] $s = -1 + (qa/V)^2[haJ_0(ha)/J_1(ha)]\Delta + O(\Delta^2) \cong -1$. Consequently, the φ-dependent terms containing $(1+s)J_2(hr)$ and $(1+s)K_2(qr)$ in the expressions (2) and (3) are negligible. Hence, the transverse component E_y or E_x will be zero if $\varphi_0 = 0$ or $\pi/2$, respectively. In addition, we have $h, q \ll \beta$, so the longitudinal component E_z is small. Thus, an exact HE_{11} mode with quasi-linear polarization of a conventional weakly guiding fiber can be approximated by a LP_{01} mode [1]. The electric field in the LP_{01} mode is given by $\mathbf{E} = F\hat{\mathbf{e}}e^{i(\omega t-\beta z)}$, where $F = \mathscr{A}J_0(hr)$ for $r < a$ and $F = \mathscr{A}[J_0(ha)/K_0(qa)]K_0(qr)$ for $r > a$. The polar-

ization vector $\hat{\mathbf{e}}$ can be chosen as $\hat{\mathbf{e}} = \hat{\mathbf{x}}$ or $\hat{\mathbf{e}} = \hat{\mathbf{y}}$. The intensity distribution of the LP_{01} mode is cylindrically symmetric.

In Fig. 1, we plot the total intensity $|E|^2$ and the x-component intensity $|E_x|^2$ of the electric field in an exact fundamental mode HE_{11} with a quasi-linear polarization, along the x direction, for the parameters of a conventional weakly guiding fiber. As seen, the transverse profiles of $|E|^2$ and $|E_x|^2$ are indistinguishable. Thus the polarization of the field is almost completely linear. We also observe that the two profiles are almost perfectly cylindrically symmetric.

We now study the case of vacuum-clad *sub-wavelength-diameter* fibers, where the relations $\Delta \ll 1$ and $a > \lambda$ are not satisfied. In this case, the factor $1 + s$ is not negligible. More importantly, the decay parameter qa of the evanescent wave may become sufficiently small that $K_1(qa)$ and $K_2(qa)$ are much larger than $K_0(qa)$. Hence, the terms containing $K_1(qr)$ and $K_2(qr)$ in the expressions (3) may become significant in the outer vicinity of the fiber surface. Due to the factor $K_1(qr)$, the longitudinal component E_z outside the fiber may become substantial. Due to the factor $K_2(qr)$, the terms containing the trigonometric functions $\cos(2\varphi - \varphi_0)$ and $\sin(2\varphi - \varphi_0)$ in the expressions (3) may become significant. These terms lead to the azimuthal dependences of the transverse components (E_x, E_y) of the field outside the fiber. In addition, when qa is small and n_1 is much different from n_2, the parameter h may be-
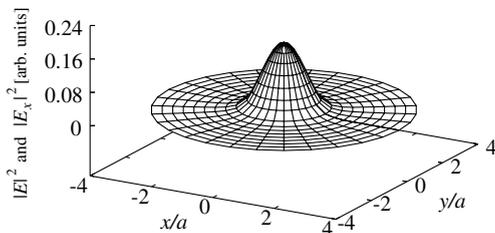

Fig. 1. Total intensity $|E|^2$ and x-component intensity $|E_x|^2$ of the electric field in an exact fundamental mode HE_{11} with a quasi-linear polarization, along the x direction, for the parameters of a conventional weakly guiding fiber. The two profiles are indistinguishable because the intensities of the y and z components of the field are negligible. The parameters used: $a = 4$ μm, $\lambda = 1.3$ μm, $n_1 = 1.4469$, $n_2 = 1.4419$, and $\varphi_0 = 0$.

come comparable to (or even larger than) the parameter β. Due to this fact, the component E_z of the field inside the fiber may also be not negligible compared to the components (E_x, E_y), respectively, see Eqs. (2). Thus the longitudinal component E_z may be substantial in both regions $r < a$ and $r > a$. So we see that the properties of the exact fundamental mode HE_{11} may become substantially different from the linearly polarized mode LP_{01}.

To demonstrate the features of vacuum-clad *subwavelength-diameter* fibers, we perform numerical calculations. The single-mode condition for vacuum-clad silica-core fibers requires that $a/\lambda < 0.36$, that is, the fiber radius be about three times smaller than the light wavelength. We consider the case where the fiber radius a is small compared not only to the light wavelength but also to the evanescent-wave penetration length $\Lambda = 1/q$. Such thin fibers can be used to trap atoms. Indeed, it has been shown that the optical force of a red-detuned evanescent wave around an optical fiber can balance the centrifugal force under the condition $qa = a/\Lambda < 0.93$ and that this condition can be achieved for vacuum-clad silica-core fibers with $a/\lambda < 0.28$ [6]. We study such thin fibers in the rest of this paper.

To be specific, we choose the fiber radius $a = 0.2$ μm and the light wavelength $\lambda = 1.3$ μm for simulations. The corresponding refractive indices of the silica core and the vacuum-clad are $n_1 \cong 1.4469$ and $n_2 = 1$, respectively. The solution of the exact eigenvalue equation (1) yields $ha \cong 1.0075$, $qa \cong 0.0827$, and $\beta a \cong 0.9702$. The normalized size parameter is $V = ka\sqrt{n_1^2 - n_2^2} \cong 1.011 < 2.405$, indicating that the considered fiber is a single-mode fiber. For the above parameters, we find $s \cong -0.9937$. The penetration length of the evanescent wave is $\Lambda \cong 12a$, large compared to the fiber radius [6]. Because of this, a majority of the field intensity distribution is in the outside of the fiber [6,7].

In Fig. 2, we plot the total intensity $|E|^2$ of the electric field in a fundamental mode with quasi-linear polarization. We choose the x axis as the major orientation axis of polarization ($\varphi_0 = 0$). As seen, the behaviors of the profiles inside and outside the fiber are very different from each other. A con-
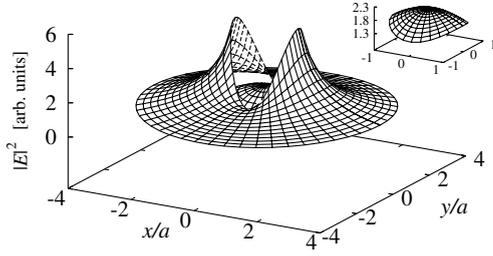
Fig. 2. Cross-section profile of the total intensity $|E|^2$ of the electric field in a fundamental mode with quasi-linear polarization. The inset shows the inner part of the profile, which corresponds to the field inside the fiber. The parameters used: $a = 0.2$ μm, $\lambda = 1.3$ μm, $n_1 = 1.4469$, $n_2 = 1$, and $\varphi_0 = 0$.
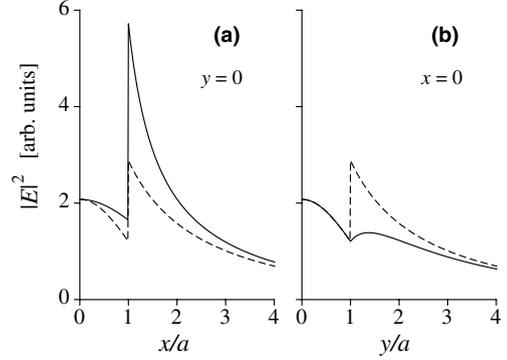

Fig. 3. Total intensity $|E|^2$ of the electric field in a fundamental mode with quasi-linear polarization as a function of x at $y = 0$ (a) and as a function of y at $x = 0$ (b). For comparison, the intensity of the electric field in the corresponding approximate mode LP_{01} is shown by the dashed lines. The parameters for this figure are the same as those for Fig. 2.

spicuous discontinuity of the field intensity is observed at the fiber surface. This discontinuity is due to the boundary condition for the normal (radial) component E_r of the electric field. The high contrast between the refractive indices n_1 and n_2 of the silica core and the vacuum-clad, respectively, makes this effect dramatic.

As seen from Fig. 2, the spatial distribution of the field intensity is not cylindrically symmetric at all. A strong dependence of the field intensity on the azimuthal angle is observed in the outer vicinity of the fiber surface. This dependence is due to the terms $w K_1^2(qr) \cos[2(\varphi - \varphi_0)]$ and $f_p K_0(qr) K_2(qr) \cos[2(\varphi - \varphi_0)]$ in Eq. (5). These terms are substantial because the small magnitude of the parameter $qa \cong 0.0827$ makes $K_1(qr)$ and $K_2(qr)$ dominant over $K_0(qr)$ in the vicinity of the fiber surface. Indeed, we have $K_1(qa)/K_0(qa) \cong 4.6$ and $K_2(qa)/K_0(qa) \cong 111.7$. In the inner vicinity of the fiber surface, the azimuthal dependence of the field intensity is moderate.

To get a look at the spatial distributions of the field along different radial directions, we replot in Fig. 3 the intensity $|E|^2$ of Fig. 2 as a function of x at $y = 0$ (as a function of r at $\varphi = 0$) and as a function of y at $x = 0$ (as a function of r at $\varphi = \pi/2$). For comparison, we plot by the dashed lines the intensity $|E_{LP}|^2$ of the corresponding approximate mode LP_{01}, which is given by $|E_{LP}|^2 = g_{in} J_0^2(hr)$ for $r < a$ and $|E_{LP}|^2 = g_{out} K_0^2(qr)$ for $r > a$. The comparison between the region $x/a > 1$ of Fig. 3(a) and the region $y/a > 1$ of Fig. 3(b) shows that, outside the fiber, $|E|^2$ de-

cays along the x direction faster than along the y direction. We observe that the radial dependence of $|E|^2$ along the y direction has a small peak in the outer vicinity of the fiber surface. Far away from the fiber surface, the decays of $|E|^2$ along the x and y directions tend to have the same behavior as that of the intensity $|E_{LP}|^2$ of the approximate mode LP_{01}. The comparison between the region $x/a < 1$ of Fig. 3(a) and the region $y/a < 1$ of Fig. 3(b) shows that, inside the fiber, $|E|^2$ decreases along the x direction slower than along the y direction. A discontinuity of $|E|^2$ is observed at the fiber surface in the x direction, but not in the y direction.

To get insight into the field components of the fundamental mode, we plot in Fig. 4 the cross-section profiles of the intensities $|E_x|^2$, $|E_y|^2$, and $|E_z|^2$ of the Cartesian-coordinate components of the electric field. In addition, we plot in Fig. 5 these intensities as functions of the azimuthal angle φ. The comparison between the scales of the vertical axes of Fig. 4(a)–(c) shows that the intensity $|E_y|^2$ of the minor transverse component E_y and the intensity $|E_z|^2$ of the longitudinal component E_z are weaker than the intensity $|E_x|^2$ of the major transverse component E_x. However, $|E_y|^2$ and $|E_z|^2$ are not negligible at all. Therefore, the alignment of the total electric field vector $\mathbf{E} = E_x \hat{\mathbf{x}} + E_y \hat{\mathbf{y}} + E_z \hat{\mathbf{z}}$ may be substantially deviated from the
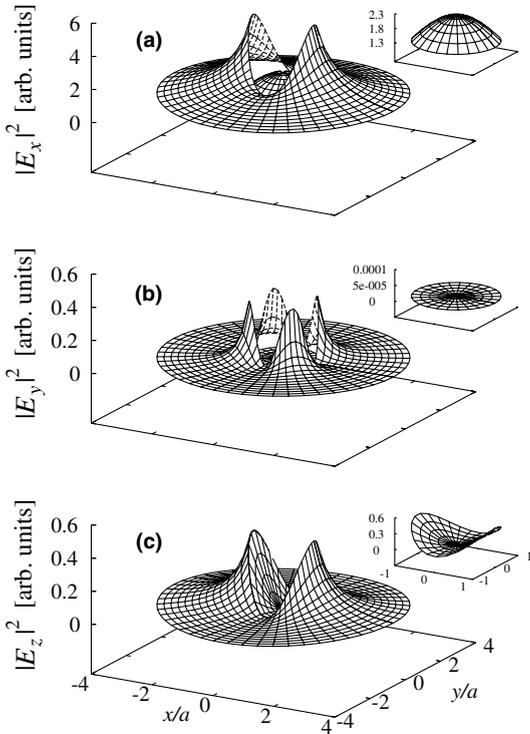
Fig. 4. Cross-section profiles of the intensities $|E_x|^2$, $|E_y|^2$, and $|E_z|^2$ of the Cartesian-coordinate components of the electric field in a fundamental mode with quasi-linear polarization. The insets show the inner parts of the profiles, which correspond to the field inside the fiber. The parameters for this figure are the same as those for Fig. 2.
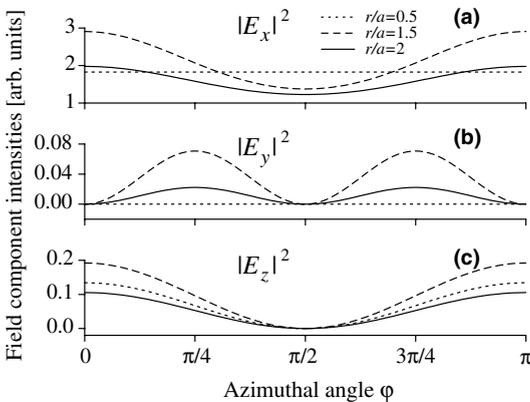

Fig. 5. Azimuthal profiles of the intensities $|E_x|^2$, $|E_y|^2$, and $|E_z|^2$ of the Cartesian-coordinate components of the electric field in a fundamental mode with quasi-linear polarization. The parameters for this figure are the same as those for Fig. 2.

major orientation axis x of polarization. According to Eqs. (2) and (3), the major and minor transverse components E_x and E_y of the electric field have the same phase. Therefore, the vector orientation of the total transverse component $\mathbf{E}_\perp = E_x\hat{\mathbf{x}} + E_y\hat{\mathbf{y}}$ does not vary in time. Thus the transverse component $\mathbf{E}_\perp$ of the field is linearly polarized with respect to the time evolution at each fixed spatial point (x, y). Meanwhile, the phase of the longitudinal component E_z differs from that of the transverse components E_x and E_y by $\pi/2$. Due to this phase difference, the total electric field $\mathbf{E}$ rotates elliptically with time, in a plane parallel to the fiber axis z.

The inset in Fig. 4(a) and the dotted curve in Fig. 5(a) show that, inside the fiber, $|E_x|^2$ practically does not vary with φ. The inset in Fig. 4(b) and the dotted curve in Fig. 5(b) show that, inside the fiber, $|E_y|^2$ is negligibly small, so the orientation of the vector $\mathbf{E}_\perp$ almost coincides with the x axis. Thus the total transverse component $\mathbf{E}_\perp$ is not only linearly polarized with respect to the time evolution at each fixed local point but also is almost linearly polarized in the space inside the fiber.

The main profiles in Figs. 4(a) and (b) as well as the dashed and solid curves in Figs. 5(a) and (b) show that, outside the fiber, $|E_x|^2$ and $|E_y|^2$ substantially depend on φ. This behavior is quite different from the behavior of the field inside the fiber.

Figs. 4, 5(c) show that the longitudinal component intensity $|E_z|^2$ is substantial not only in the outer vicinity of the fiber surface but also in the inner vicinity, unlike the minor transverse component intensity $|E_y|^2$. In addition, $|E_z|^2$ substantially varies with φ not only outside but also inside the fiber, unlike the major transverse component intensity $|E_x|^2$. The azimuthal dependence of $|E_z|^2$ is profound in both sides of the fiber surface because E_z is proportional to $\cos(\varphi - \varphi_0)$, see Eqs. (2) and (3).

At each fixed spatial point, the vector orientation of the total transverse component $\mathbf{E}_\perp$ of the electric field does not, as discussed earlier, vary in time. However, the orientation of $\mathbf{E}_\perp$ may vary in space, especially in the outer vicinity of the fiber surface, where the minor transverse component E_y is substantial. We plot in Fig. 6 the orientation an-
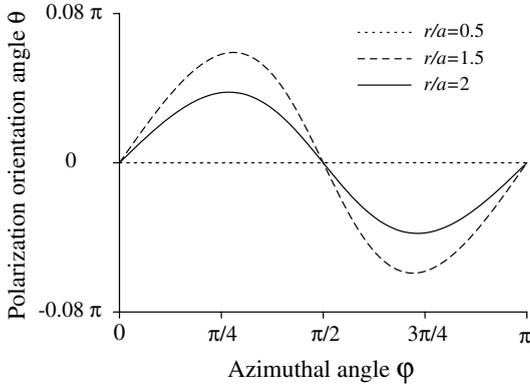
Fig. 6. Orientation angle $\theta = \arctan[\mathrm{Re}(E_y)/\mathrm{Re}(E_x)]$ of the transverse component $\mathbf{E}_\perp$ of the electric field in a fundamental mode with quasi-linear polarization. The parameters for this figure are the same as those for Fig. 2.

gle $\theta = \arctan[\mathrm{Re}(E_y)/\mathrm{Re}(E_x)]$ of $E_\perp$ as a function of φ. The dotted curve in Fig. 6 shows that, inside the fiber, the orientation angle θ almost does not vary with φ. This feature confirms that the total transverse component $\mathbf{E}_\perp$ inside the fiber is almost linearly polarized in space. It is due to the fact that the φ-dependent terms in the expressions for the transverse components inside the fiber are negligible. Meanwhile, the dashed and solid curves in Fig. 6 show that, outside the fiber, the orientation angle θ does vary in space. For $r/a = 1.5$, the maximal azimuthal variation of θ is about 0.06π (see the dashed curve). The comparison between the solid and dashed curves in Fig. 6 shows that, when r increases from a, the azimuthal variation of θ reduces. These features are due to the fact that the ratio between the factors $K_2(qr)$ and $K_0(qr)$ of the φ-dependent and -independent terms is large for $qr \ll 1$ but monotonically reduces to unity with increasing r.

3. Fundamental mode with rotating polarization

We now study a fundamental mode with rotating (circulating) polarization. In the cylindrical coordinates, the solutions of Maxwell's equations for the cylindrical components of the electric field $\mathbf{E}$ in such a mode are given by [1]

$$E_r = F_r e^{\pm i\varphi} e^{i(\omega t - \beta z)},$$
$$E_\varphi = \pm F_\varphi e^{\pm i\varphi} e^{i(\omega t - \beta z)}, \qquad (6)$$
$$E_z = F_z e^{\pm i\varphi} e^{i(\omega t - \beta z)}.$$

Here the functions F_j ($j = r, \varphi, z$) describe the radial dependences of the field components. They are defined, for $r < a$, as

$$F_r = -iA\frac{\beta}{2h}[(1-s)J_0(hr) - (1+s)J_2(hr)],$$
$$F_\varphi = A\frac{\beta}{2h}[(1-s)J_0(hr) + (1+s)J_2(hr)], \qquad (7)$$
$$F_z = AJ_1(hr),$$

and, for $r > a$, as

$$F_r = -iA\frac{\beta}{2q}\frac{J_1(ha)}{K_1(qa)}[(1-s)K_0(qr) + (1+s)K_2(qr)],$$
$$F_\varphi = A\frac{\beta}{2q}\frac{J_1(ha)}{K_1(qa)}[(1-s)K_0(qr) - (1+s)K_2(qr)],$$
$$F_z = A\frac{J_1(ha)}{K_1(qa)}K_1(qr). \qquad (8)$$

The upper (lower) sign in Eqs. (6) corresponds to the clockwise (counterclockwise) circulation of photons around the z axis. According to Eqs. (6), we have $|E_j| = |F_j|$. According to Eqs. (7) and (8), the functions F_j are independent of the azimuthal angle φ. Hence, the intensities $|E_j|^2$ of the cylindrical-coordinate components of the field are independent of φ, and so is the total intensity $|E|^2$ of the electric field.

According to Eqs. (7) and (8), we have $F_r/|F_r| = -iF_\varphi/|F_\varphi|$. Then, it follows from Eqs. (6) that $E_r/|E_r| = \mp iE_\varphi/|E_\varphi|$, that is, the two complex quadratures E_r and E_φ have a difference of $\pi/2$ between their phases. Therefore, the polarization of the total transverse component $\mathbf{E}_\perp = E_r\hat{\mathbf{r}} + E_\varphi\hat{\boldsymbol{\varphi}}$ of the field is either circular or elliptical. With increasing time, the real part of the complex amplitude vector $\mathbf{E}_\perp$ rotates along a circle or an ellipse. The semimajor and semiminor axes of the ellipse are aligned along the unit vectors $\hat{\mathbf{r}}$ and $\hat{\boldsymbol{\varphi}}$, respectively, and are equal to $|E_r| = |F_r|$ and $|E_\varphi| = |F_\varphi|$, respectively. When $|E_r| \cong |E_\varphi|$, the elliptical polarization of the transverse component of the field becomes almost circular.

We can easily calculate the total intensity $|E|^2$ of the electric field in a fundamental mode with rotating polarization. For the field inside the fiber, we obtain

$$|E|^2 = 2g_{in}[J_0^2(hr) + uJ_1^2(hr) + fJ_2^2(hr)]. \qquad (9)$$

For the field outside the fiber, we get

$$|E|^2 = 2g_{out}[K_0^2(qr) + wK_1^2(qr) + fK_2^2(qr)]. \qquad (10)$$

The terms $J_0^2(hr)$ and $K_0^2(qr)$ in the expressions (9) and (10), respectively, correspond to the total intensity of the electric field in the mode LP_{01}. The other terms describe the deviations of the exact fundamental mode HE_{11} with rotating polarization from the approximate mode LP_{01}. The comparison between Eqs. (4) and (9) and between Eqs. (5) and (10) shows that the total intensity of the electric field in a fundamental mode with rotating polarization is the sum of the corresponding intensities for two constituent modes with quasi-linear polarizations. The φ-dependent terms cancel each other and therefore do not appear in Eqs. (9) and (10).

The above expressions are mathematically valid for the fundamental mode with rotating polarization of a fiber with an arbitrary core radius a and an arbitrary pair of refractive indices $n_1 > n_2$. To demonstrate the features of vacuum-clad *sub-wavelength-diameter* fibers, we perform numerical calculations for the parameters of the previous section, namely, for $a = 0.2$ μm, $\lambda = 1.3$ μm, $n_1 \cong 1.4469$, and $n_2 = 1$.

In Fig. 7, we plot the cross-section profile of the total intensity $|E|^2$ of the electric field in a fundamental mode with rotating polarization. As seen, $|E|^2$ is azimuthally independent, that is, is cylindrically symmetric. The discontinuity of the field at the fiber surface, created by the boundary condition and the high contrast between n_1 and n_2, divides the profile into two parts. The inner part of the profile is hidden behind the outer part and is shown separately in the inset of the figure.

In Fig. 8, we plot by the solid line the total intensity $|E|^2$ of the electric field as a function of the radial distance r. For comparison, we plot by the dashed line the intensity $|E_{LP}|^2$ of the corresponding approximate mode LP_{01}, which is given by $|E_{LP}|^2 = 2g_{in}J_0^2(hr)$ for $r < a$ and
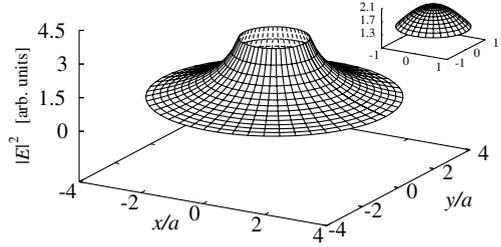

Fig. 7. Cross-section profile of the total intensity $|E|^2$ of the electric field in a fundamental mode with rotating polarization. The inset shows the inner part of the profile, which corresponds to the field inside the fiber. The parameters for this figure are the same as those for Fig. 2.
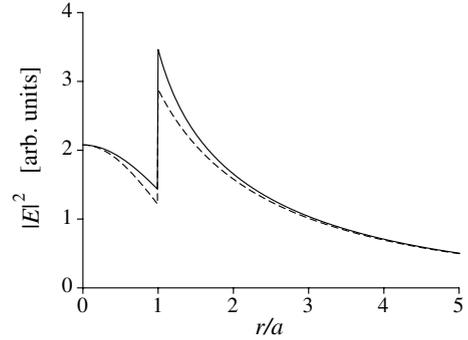

Fig. 8. Radial dependence of the total intensity $|E|^2$ of the electric field in a fundamental mode with rotating polarization (solid line). For comparison, the intensity $|E_{LP}|^2$, obtained for the corresponding approximate mode LP_{01}, is plotted by the dashed line. The parameters for this figure are the same as those for Fig. 2.

$|E_{LP}|^2 = 2g_{out}K_0^2(qr)$ for $r > a$. As seen, the difference between $|E|^2$ and $|E_{LP}|^2$ is small but not negligible in the region $0.3 < r/a < 3$. Inside the fiber, $|E|^2$ (solid curve) decreases slower than $|E_{LP}|^2$ (dashed curve). Such a behavior of $|E|^2$ is due to the contributions of the last two terms in Eq. (9). These terms contain the functions J_1 and J_2, which increase in the region of small argument. In the outer vicinity of the fiber surface, $|E|^2$ (solid curve) decays faster than $|E_{LP}|^2$ (dashed curve). Such a behavior of $|E|^2$ is due to the contributions of the additional terms $wK_1^2(qr)$ and $fK_2^2(qr)$ in Eq. (10), which decay faster than the basic term $K_0^2(qr)$ in the region of small argument. When r/a

is large enough ($r/a > 3$), the difference between $|E|^2$ and $|E_{LP}|^2$ can be neglected.

The intensities $|E_r|^2$, $|E_\varphi|^2$, and $|E_z|^2$ of the cylindrical-coordinate components of the field are determined by the cylindrically symmetric functions $|F_r|^2$, $|F_\varphi|^2$, and $|F_z|^2$, respectively. We plot these intensities as functions of r in Fig. 9. As seen, the field intensity distributions inside ($r/a < 1$) and outside ($r/a > 1$) the fiber have very different behaviors. Due to the boundary condition and the high contrast between the refractive indices of the silica core and the vacuum-clad, the normal (radial) component E_r has a conspicuous discontinuity at the fiber surface. The tangential components E_φ and E_z are, however, continuous.

Unlike the intensities of the cylindrical-coordinate components E_r, E_φ, and E_z, the intensities of the Cartesian-coordinate transverse components E_x and E_y are, in general, not cylindrically symmetric. In Fig. 10, we plot the cross-section profiles of the intensities $|E_x|^2$, $|E_y|^2$, and $|E_z|^2$. In addition, we plot these intensities in Fig. 11 as functions of φ.

The insets in Figs. 10(a) and (b) as well as the dotted curves in Figs. 11(a) and (b) show that, inside the fiber, $|E_x|^2$ and $|E_y|^2$ are almost equal to each other and practically do not vary with φ. The reason is that the φ-dependent terms in the expressions for F_r and F_φ in Eqs. (7) are negligible. Because of this, we have $F_r \cong -iF_\varphi$ and, conse-
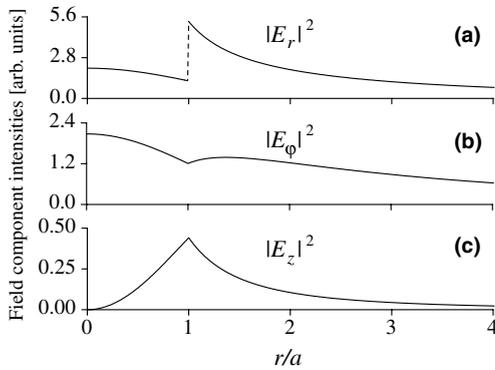

Fig. 9. Intensities $|E_r|^2$, $|E_\varphi|^2$, and $|E_z|^2$ of the cylindrical-coordinate components of the field in a fundamental mode with rotating polarization. The parameters for this figure are the same as those for Fig. 2.
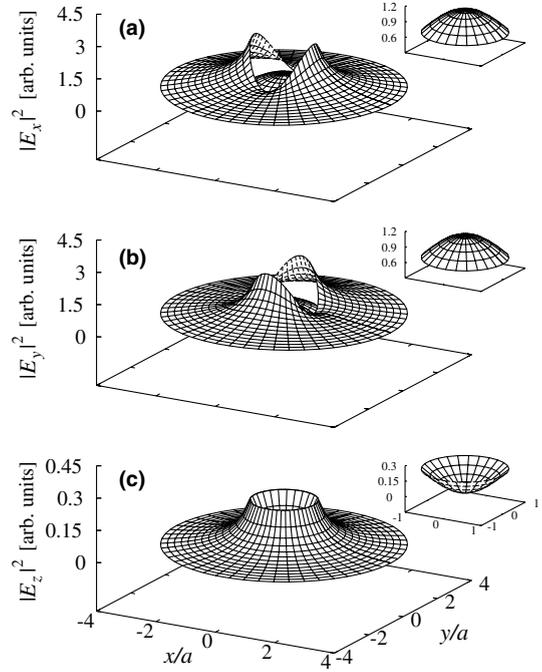

Fig. 10. Cross-section profiles of the intensities $|E_x|^2$, $|E_y|^2$, and $|E_z|^2$ of the Cartesian-coordinate components of the electric field in a fundamental mode with rotating polarization. The insets show the inner parts of the profiles, which correspond to the field inside the fiber. The parameters for this figure are the same as those for Fig. 2.
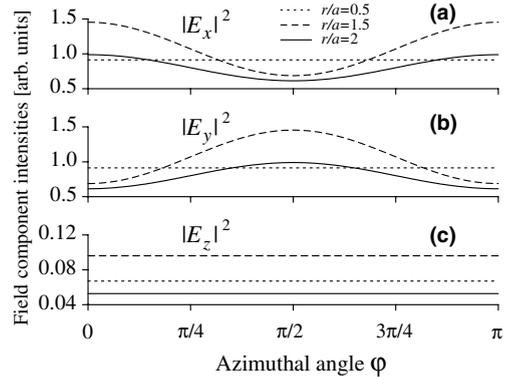

Fig. 11. Azimuthal profiles of the intensities $|E_x|^2$, $|E_y|^2$, and $|E_z|^2$ of the Cartesian-coordinate components of the electric field in a fundamental mode with rotating polarization. The parameters for this figure are the same as those for Fig. 2.

quently, $E_r \cong \mp iE_\varphi$. Hence, we find $E_x \cong -F_r e^{i(\omega t - \beta z)}$, $E_y \cong \pm iF_r e^{i(\omega t - \beta z)}$, and consequently $E_x \cong \mp iE_y$. Thus the two orthogonal quadratures

E_r and E_φ as well as E_x and E_y have almost equal magnitudes and a relative phase difference of $\pi/2$. This indicates that, inside the fiber, the total transverse component $\mathbf{E}_\perp$ of the field is almost circularly polarized.

The main profiles in Figs. 10(a) and (b) as well as the dashed and solid curves in Figs. 11(a) and (b) show that, outside the fiber, the intensities of the transverse components E_x and E_y are different from each other and substantially vary with φ. The comparison between the dashed lines and the solid lines in Figs. 11(a) and (b) shows that the azimuthal dependences of $|E_x|^2$ and $|E_y|^2$ outside the fiber reduce with increasing r.

The terms $\pm(1 + s)K_2(qr)$ in Eqs. (8) lead to $|F_r| \neq |F_\varphi|$ and, hence, to $|E_r| \neq |E_\varphi|$. Due to the substantial difference between $|E_r|$ and $|E_\varphi|$ in the outer vicinity of the fiber surface, the polarization of the transverse component $\mathbf{E}_\perp$ of the field in this region is truly elliptical. We recall that the axes of the elliptical circulation orbit are aligned along the unit vectors $\hat{\mathbf{r}}$ and $\hat{\boldsymbol{\varphi}}$. Consequently, the orientation of the orbit varies with increasing φ. We also recall that the lengths of the axes of the ellipse are equal to $|E_r| = |F_r|$ and $|E_\varphi| = |F_\varphi|$. Hence, the ellipticity of the orbit is proportional to the factor $(1 + s)K_2(qr)/(1 - s)K_0(qr)$. This factor reduces with increasing r. Thus both the orientation and the ellipticity of the orbit of polarization circulation vary in space. This behavior is different from the case of conventional light beams with elliptical or circular polarization. Furthermore, we note that the ellipticity of the orbit of polarization circulation does not depend on φ. This indicates that the orbit rotates circularly in space.

Figs. 10, 11(c) show that the longitudinal component intensity $|E_z|^2$ is perfectly cylindrically symmetric, as expected, in the whole cross-section plane. Although $|E_z|^2$ is small compared to $|E_x|^2$ and $|E_y|^2$, it is not negligible in the vicinity of the fiber surface.

4. Conclusions

We have studied the properties of the field in the fundamental mode HE_{11} of a vacuum-clad *subwavelength-diameter* optical fiber using the exact solutions of Maxwell's equations. We have obtained simple analytical expressions for the total intensity of the electric field and have identified the origin of the deviations of the exact fundamental mode HE_{11} from the approximate mode LP_{01}. We have shown that the thin thickness of the fiber and the high contrast between the refractive indices of the silica core and the vacuum-clad substantially modify the intensity distributions and the polarization properties of the field and its components, especially in the vicinity of the fiber surface.

We have examined the case of a fundamental mode with quasi-linear polarization. We have shown that a substantial azimuthal dependence of the total intensity is observed in the vicinity of the fiber surface. The transverse component of the field is linearly polarized in time at each fixed local point. However, the total electric field vector rotates elliptically with time, in a plane parallel to the fiber axis. Inside the fiber, the transverse component is not only linearly polarized in time but also almost linearly polarized in space. Outside the fiber, the orientation angle of the transverse component of the field varies in space.

We have also studied the case of a fundamental mode with rotating (circulating) polarization. We have shown that the total intensity is azimuthally independent, that is, is cylindrically symmetric. We have found that the total intensity of the electric field outside the fiber decays faster than that of the approximate mode LP_{01}. The difference between the exact and approximate modes is relatively small in the case of rotating polarization. Consequently, the underlying physics of the optical potential of the evanescent wave around a vacuum-clad subwavelength-diameter fiber is basically the same as that of the approximate mode LP_{01}. However, the magnitude of the difference is not negligible in the vicinity of the fiber surface. Therefore, the use of the exact solutions of Maxwell's equations is required in a systematic quantitative treatment for a thin fiber. We have shown that, inside the fiber, the total transverse component of the field is almost circularly polarized. In the outer vicinity of the fiber surface, the polarization of the transverse component of the field is elliptical. In this region, the orientation of the orbit of polarization circulation rotates in

space while the ellipticity of the orbit reduces with increasing radial distance. This is different from the case of conventional light beams with elliptical or circular polarization. Our results are helpful for studying and developing new miniaturized high-performance photonic devices. One of the promising applications of the field around the subwavelength-diameter fiber is trapping and guiding of neutral atoms by the optical force of the evanescent field.

Acknowledgements

References

[1] See, for example A. Yariv, Optical Electronics, CBS College, New York, 1985;
D. Marcuse, Light Transmission Optics, Krieger, Malabar, FL, 1989;
A.W. Snyder, J.D. Love, Optical Waveguide Theory, Chapman and Hall, New York, 1983.

[2] J. Bures, R. Ghosh, J. Opt. Soc. A 16 (1999) 1992.

[3] T.A. Birks, W.J. Wadsworth, P.St.J. Russell, Opt. Lett. 25 (2000) 1415;
S.G. Leon-Saval, T.A. Birks, W.J. Wadsworth, P.St.J. Russell, M.W. Mason, Conference on Lasers and Electro-Optics (CLEO), Technical Digest, Postconference Edition, Optical Society of America, Washington, DC 2004, Paper CPDA6.

[4] M.J. Levene, J. Korlach, S.W. Turner, M. Foquet, H.G. Craighead, W.W. Webb, Science 299 (2003) 682.

[5] L. Tong, R.R. Gattass, J.B. Ashcom, S. He, J. Lou, M. Shen, I. Maxwell, E. Mazur, Nature 426 (2003) 816.

[6] V.I. Balykin, K. Hakuta, Fam Le Kien, J.Q. Liang, M. Morinaga, Phys. Rev. A 70 (2004) 011401(R);
V.I. Balykin, Fam Le Kien, J.Q. Liang, M. Morinaga, K. Hakuta, Atom spinning around an optical fiber: bound states and guiding, CLEO/IQEC and PhAST Technical Digest on CD-ROM, Optical Society of America, Washington, DC 2004, Presentation ITuA7.

[7] L. Tong, J. Lou, E. Mazur, Optics Express 12 (2004) 1025.

[8] B.Z. Katsenelenbaum, Zh. Tekh. Fiz. XIX (1949) 1168 (in Russian);
B.Z. Katsenelenbaum, Zh. Tekh. Fiz. XIX (1949) 1182 (in Russian).

[9] H. Nha, W. Jhe, Phys. Rev. A 56 (1997) 2213.

[10] W. Zakowicz, M. Janowicz, Phys. Rev. A 62 (2000) 013820.

[11] V.V. Klimov, M. Ducloy, Phys. Rev. A 69 (2004) 013812.

[12] J.C. Knight, G. Cheung, F. Jacques, T.A. Birks, Opt. Lett. 22 (1997) 1129;
G. Kakarantzas, T.E. Dimmick, T.A. Birks, R. Le Roux, P.St.J. Russell, Opt. Lett. 26 (2001) 1137;
M. Cai, K. Vahala, Opt. Lett. 26 (2001) 884.